Nuclear Effects in the Production of π^+ and π^- by Protons on Nuclei

Richard R. Silbar*
Los Alamos Scientific Laboratory, University of California, Los Alamos, New Mexico 87544

Morton M. Sternheim†
Department of Physics and Astronomy, University of Massachusetts, Amherst, Massachusetts 01002

(Received 13 April 1973)

We have modified an earlier semiclassical model of pion production by protons on nuclei by including various nuclear physics corrections. In addition to allowing for $p\,n$ charge exchange and realistic nuclear densities, we have corrected the two-body input cross sections for the effects of the Pauli principle, Fermi motion, and nuclear optical potentials. The agreement with experiment is similar to that obtained earlier. Ambiguities arising from the nuclear corrections are found to be larger than the effects of moderate variations of the nuclear surface parameters.

I. INTRODUCTION

In a recent paper[1] we used a semiclassical model to analyze the data of Cochran *et al.* on the production of pions from nuclei by 740-MeV protons.[2] Considering the simplicity of the model, the success in reproducing the general features of the data was rather striking. In this paper we consider the effects on the model of making various nuclear physics corrections.

The motivation for this work was already stated in Ref. 1 (hereafter referred to as I): With an improved calculation of this sort one might hope to extract new information concerning the nuclear surface from pion-production experiments.[3] Unfortunately, on considering the ambiguities present in making nuclear corrections, we do not now feel that this is possible. The ambiguities which lead to this negative conclusion will become apparent below.

On the other hand, a positive result of our investigations is that pion production from nuclei provides a useful testing ground for studying how the nuclear medium—through the Fermi motion, the Pauli exclusion principle, and the various nuclear potentials—can affect processes which take place within it. These effects, of course, are of importance throughout pion-nucleus physics. One of the byproducts of the present calculation is a more meaningful fit of the pion-absorption cross section, $\sigma_{\pi,\mathrm{abs}}(T)$, now quite a bit changed from the fit in I. That is to say, taking account of the corrections due to the nuclear medium is quite important in extracting nuclear-averaged quantities.

The outline of the paper is as follows. Section II reviews the semiclassical model of I and extends it to include charge exchange for the incident nucleon and a nonuniform nuclear density. Section III discusses the five cross sections needed for the calculation. Four of these are known but must be corrected for the nuclear effects mentioned above. The fifth, $\sigma_{\pi,\mathrm{abs}}(T)$, is obtained by a fitting procedure. Numerical results for pion-production cross sections are presented in Sec. IV. The comparison with data is not better here than in I; indeed, the predicted π^+/π^- ratio is not as good. Section IV also shows the relative importance of each of the corrections treated here. Finally, Sec. V gives a concluding summary.

II. SEMICLASSICAL MODEL

We assume that the incident nucleon travels in a straight line within the nucleus to some point $\vec{r}$. There it makes a pion of kinetic energy T at an angle θ to the incident direction via the one-step reaction $NN \to NN\pi$. The pion then moves out of the nucleus in a straight line. Both the incident-nucleon and outgoing-pion fluxes are attenuated by interactions with the nuclear medium.[3,4] Also, the relative populations of the nucleon and pion charge states are altered by charge-exchange processes.[1]

The numbers of protons and neutrons, N_p and N_n, reaching the production point are determined by the differential equations

$$\begin{aligned} N_p' &= -(\lambda_a^N + \lambda_{x,n}^N + \lambda_{\Delta,p}) N_p + \lambda_{x,p}^N N_n \,, \\ N_n' &= -(\lambda_a^N + \lambda_{x,p}^N + \lambda_{\Delta,n}) N_n + \lambda_{x,n}^N N_n \,. \end{aligned} \tag{1}$$

Here $\lambda_a^N = A\rho\sigma_{N,\mathrm{abs}}$ is the inverse mean free path for absorption of nucleons, assumed to be the same for protons and neutrons. It corresponds to those interactions with target nucleons which leave the incident nucleons without sufficient energy to make pions. The quantities $\lambda_{x,n}^N = N\rho\sigma_{N,\mathrm{exch}}$ and $\lambda_{x,p}^N = Z\rho\sigma_{N,\mathrm{exch}}$ are the inverse mean free paths for the charge-exchange reactions $pn \to np$ and $np \to pn$, respectively. Finally, the quantities

$$\begin{aligned} \lambda_{\Delta,p} &= (Z + \tfrac{1}{2} N)\rho\sigma_{\mathrm{iso}} \,, \\ \lambda_{\Delta,n} &= (N + \tfrac{1}{2} Z)\rho\sigma_{\mathrm{iso}} \end{aligned} \tag{2}$$

are the inverse mean free paths for pion production according to the isobar model.[5] For the nuclear density, ρ, we use a Saxon-Woods form with parameters obtained from electron scattering[6]:

$$\rho(\vec{r}) = \rho_0[1+\exp(r-r_0)/a]^{-1}, \qquad \int \rho\, d^3r = 1. \tag{3}$$

The analogous transport equations for the outgoing pions are

$$\begin{aligned} N_+' &= -\lambda_a N_+ - \lambda_{x,n} N_+ + \lambda_{x,p} N_0, \\ N_0' &= -\lambda_a N_0 - (\lambda_{x,n}+\lambda_{x,p}) N_0 + \lambda_{x,n} N_+ + \lambda_{x,p} N_-, \\ N_-' &= -\lambda_a N_- - \lambda_{x,p} N_- + \lambda_{x,n} N_0. \end{aligned} \tag{4}$$

Here $\lambda_a = A\rho\sigma_{\pi,\mathrm{abs}}(T)$, $\lambda_{x,n} = N\rho\sigma_{\pi,\mathrm{exch}}(T)$, and $\lambda_{x,p} = Z\rho\sigma_{\pi,\mathrm{exch}}(T)$ correspond to pion absorption, pion charge exchange on neutrons, and pion charge exchange on protons, respectively.

Both sets of transport equations are of the form

$$N' = B\rho N, \tag{5}$$

where B is a *constant* square matrix and N is a column matrix. The solution to Eq. (5) is[7]

$$N(\vec{r}) = \exp[B\mathcal{R}(\vec{r})]N(0), \tag{6}$$

where

$$\mathcal{R}(\vec{r}) = \int \rho[\vec{r}'(s)]\, ds \tag{7}$$

is an integral along the appropriate path length. It goes from $(0, 0, -\infty)$ to the production point $\vec{r} = (x, y, z)$ for the nucleons and from $\vec{r}$ to ∞ along the direction θ for the pions. By standard methods, we can find a constant matrix S such that $\tilde{B} = S^{-1}BS$ is diagonal. Then

$$N(\vec{r}) = S\exp[\tilde{B}\mathcal{R}(\vec{r})]S^{-1}N(0) \tag{8}$$

or

$$N_i(\vec{r}) = \sum_j M_{ij}(\vec{r}) N_j(0), \tag{9}$$

where

$$M_{ij}(\vec{r}) = \sum_k S_{ik} \exp[\tilde{B}_{kk}\mathcal{R}(\vec{r})](S^{-1})_{kj}. \tag{10}$$

The pion M_{ij}'s were given in Eqs. (7) of I for the constant nuclear density case. They are the same here but with the replacement

$$s \to \mathcal{R}(\vec{r})/\rho_0. \tag{11}$$

For the nucleons, with $N_p(0) = 1$ and $N_n(0) = 0$, we find

$$\begin{aligned} N_p &= (e^{-\alpha\mathcal{R}}/2\beta)[(\beta-\gamma)e^{\beta\mathcal{R}} + (\beta+\gamma)e^{-\beta\mathcal{R}}], \\ N_n &= (N\sigma_{N,\mathrm{exch}} e^{-\alpha\mathcal{R}}/2\beta)[e^{\beta\mathcal{R}} - e^{-\beta\mathcal{R}}], \end{aligned} \tag{12}$$

where

$$\begin{aligned} \alpha &= A(\sigma_{N,\mathrm{abs}} + \tfrac{1}{2}\sigma_{N,\mathrm{exch}} + \tfrac{3}{4}\sigma_{\mathrm{iso}}), \\ \beta &= \tfrac{1}{2}[(A\sigma_{N,\mathrm{exch}})^2 + \tfrac{1}{4}(N-Z)^2\sigma_{\mathrm{iso}}(\sigma_{\mathrm{iso}} - 4\sigma_{N,\mathrm{exch}})]^{1/2}, \\ \gamma &= \tfrac{1}{2}(N-Z)(\sigma_{N,\mathrm{exch}} - \tfrac{1}{2}\sigma_{\mathrm{iso}}). \end{aligned} \tag{13}$$

The cross section for pions of charge i, produced at $\vec{r}$ with charge j, is a sum of products of the density, the production cross section for $NN \to NN\pi$, and the various transport quantities. Explicitly,

$$\frac{d^2\sigma(\pi^i)}{dT d\Omega} = \frac{d^2\sigma_{\mathrm{iso}}}{dT d\Omega} \sum_j \int d^3\vec{r}\, \rho(\vec{r}) M_{ij}(\vec{r}) \times [N_p(\vec{r})p_j + N_n(\vec{r})n_j]. \tag{14}$$

Here the weight factors p_j and n_j are obtained from the Clebsch-Gordan coefficients of the isobar production model[5]:

$$\begin{aligned} p_+ &= \tfrac{5}{6}Z + \tfrac{1}{12}N, & n_+ &= \tfrac{1}{12}Z, \\ p_0 &= \tfrac{1}{6}Z + \tfrac{1}{3}N, & n_0 &= \tfrac{1}{3}Z + \tfrac{1}{12}N, \\ p_- &= \tfrac{1}{12}N, & n_- &= \tfrac{1}{12}Z + \tfrac{5}{6}N. \end{aligned} \tag{15}$$

III. INPUT CROSS SECTIONS

Equation (14) involves five cross sections on the right-hand side: $\sigma_{N,\mathrm{abs}}$, $\sigma_{N,\mathrm{exch}}$, $d^2\sigma_{\mathrm{iso}}/dTd\Omega$, $\sigma_{\pi,\mathrm{exch}}$, and $\sigma_{\pi,\mathrm{abs}}$. The last of these is not known and we will resort to a fitting procedure to obtain it. Values for the first four cross sections can be extracted from experimental data on reactions on free nucleons. These should be corrected for the effects of Fermi motion, the Pauli exclusion principle, and nuclear potentials. These corrections, however, are subtle (and difficult) in ways that we did not at first appreciate. One question, for example, is the meaning of a potential that is of the same order as the rest mass of the particle involved. Another is the playing off of a space-time description against a momentum-energy description without due respect for the uncertainty principle.[8] Presumably, in some future relativistic quantum-mechanical treatment these and related problems would be well under control. For now, however, we will try to do the best we can without going into unrewardingly complex detours.

A. Nucleon-Absorption Cross Section

The total pp cross section at a laboratory kinetic energy of 740 MeV is about 46 mb.[9] Of this, 13.50 $\pm$0.73 mb is π^+ production.[2] According to the isobar model,[5] the cross section for π^0 production is $(\frac{1}{6})\sigma_{\mathrm{iso}} = (\frac{1}{5})\sigma(pp \to np\pi^+) \approx 2.7$ mb.[10] The remaining 30 mb is elastic scattering.

If the incident proton scatters elastically through

a small angle, suffering only a small energy loss, it is still able to produce pions and its path is more or less correctly treated in our semiclassical model. If its energy loss, however, is 180 MeV or greater, corresponding to a laboratory scattering angle of 26° or greater, then we are one Δ half-width below the threshold for $pp \to N\Delta$, and the pion production becomes small. (Experimentally,[9] at 560 MeV π^+ and π^0 production have dropped by 62 and 74%, respectively, from their values at 740 MeV.)

The cross section for such large-angle scatterings is fairly small. To a sufficient accuracy the elastic pp differential cross section is[9]

$$d\sigma/dt = 25.9\, e^{-c|t|}\,\text{mb}/(\text{GeV}/c)^2, \tag{16}$$

where $c = 4.1$ and 4.98 $(\text{GeV}/c)^{-2}$ at 705 and 788 MeV, respectively. The cross section for np elastic scattering is similar.[9] If the energy lost by the nucleon is $\Delta E = 180$ MeV, then the corresponding squared four-momentum transfer is

$$t_{\max} = -2m\Delta E = -0.338\ (\text{GeV}/c)^2. \tag{17}$$

Thus

$$\sigma_{N,\text{abs}} = \int_{-\infty}^{t_{\max}} \left(\frac{d\sigma}{dt}\right) dt = \begin{cases} 6.5 \text{ mb at 705 MeV} \\ 4.8 \text{ mb at 788 MeV}. \end{cases} \tag{18}$$

We will use the average value,

$$\sigma_{N,\text{abs}} = 5.6 \text{ mb}. \tag{19}$$

Since this cross section is only moderately energy-dependent and relatively large energies are involved, we have not made any corrections for Fermi motion, the Pauli principle, or nuclear potentials.

Note that our value of $\sigma_{N,\text{abs}}$ is small compared to the total elastic NN cross section. By contrast, other authors[3,4] have assumed them equal. With that assumption, the pion production occurs mainly in the nuclear surface. This is, of course, less pronounced in our calculations. As we shall see, this implies that our results are not very sensitive to details of the nuclear surface, in contrast with the conclusion reached in earlier studies.[3]

B. Nucleon-Charge-Exchange Cross Section

The cross section $\sigma_{N,\text{exch}}$ corresponds to a proton scattering on a neutron with the neutron emerging with most of the momentum. Thus

$$\sigma_{N,\text{exch}} = \int_0^{\theta_m} \frac{d\sigma}{d\Omega}(pn \to np) R(\theta) d\Omega. \tag{20}$$

As in the preceding discussion, θ_m must not exceed about 26° in the lab if the neutron is to have sufficient energy to make a pion.

The Pauli principle reduces $d\sigma/d\Omega$ at small scattering angles by the factor $R(\theta)$. Following an argument given by Bethe[11] in another context, let us treat the nucleus as a Fermi gas with a Fermi momentum k_F. The struck neutron therefore has an initial laboratory momentum $\vec{k}$ which lies within a sphere of radius k_F. The final (slow) proton has momentum $\vec{k}' = \vec{k} + \vec{q}_L$, where $\vec{q}_L$ is the three-momentum transfer in the laboratory. Thus $\vec{k}'$ also lies within a sphere of radius k_F but with its center displaced by $\vec{q}_L$. The region of overlap between these two spheres is excluded by the Pauli principle. This volume then gives the reduction factor $R(\theta)$ appearing in Eq. (20),

$$R(\theta) = \frac{3}{4}\left(\frac{q_L}{k_F} - \frac{{q_L}^3}{12{k_F}^3}\right). \tag{21}$$

Note that, again, the relatively weak energy dependence of $d\sigma/d\Omega$ allows us to neglect the effects of Fermi motion and nuclear potentials.

Using $k_F = 250$ MeV/c and 649-MeV $np \to pn$ data[12] in Eq. (20) gives $\sigma_{N,\text{exch}} = 3.4$ mb. The 816-MeV data[12] gives 2.8 mb. We will use the average value

$$\sigma_{N,\text{exch}} = 3.1 \text{ mb}. \tag{22}$$

Without the Pauli-principle reduction this cross section would be about 40% larger.

C. Pion-Production Cross Section

Beder and Bendix have stated[4] that substantial corrections to the pion-production differential cross section, $d^2\sigma_{\text{iso}}/dT d\Omega$, arise from Fermi-motion averaging and the nucleon-nucleus and pion-nucleus potentials. By contrast, the Pauli principle implies only a minor reduction factor even for the fastest pions and hence can be neglected.[13]

We will use a phase-space model to derive a correction factor $F(T, \theta)$ which will multiply the experimental $pp \to np\pi^+$ differential cross sections needed in Eq. (14). We write

$$F(T,\theta) = \left(\frac{d^2\sigma}{dT d\Omega}\right)_{\text{ave}} \Big/ \left(\frac{d^2\sigma}{dT d\Omega}\right)_{\text{free}}, \tag{23}$$

where, following Beder and Bendix,[4] we average over the Fermi momentum distribution according to

$$\left(\frac{d^2\sigma}{dT d\Omega}\right)_{\text{ave}} = \frac{3}{4\pi {k_F}^3} \int_0^{k_F} d^3k \left(\frac{d^2\sigma(\vec{k})}{dT d\Omega}\right)_{\text{free}} \tag{24}$$

and

$$\left(\frac{d^2\sigma(\vec{k})}{dTd\Omega}\right)_{\text{free}} = \frac{p_{\pi,\text{lab}}}{[(p_1\cdot p_2)^2 - p_1^2 p_2^2]^{1/2}} \frac{k_{NN}}{W_{NN}} |M|^2 . \tag{25}$$

Here $\vec{k}$ is the three-momentum of the struck nucleon, p_1 and p_2 are the initial nucleon four-momenta, k_{NN} is the three-momentum of one of the nucleons in the final two-nucleon c.m. frame, c.m. frame, $W_{NN}^2 = (p_1' + p_2')^2$ is the invariant mass squared of the final NN system, and $p_{\pi,\text{lab}}$ is the pion laboratory momentum.

The phase-space model consists of taking the matrix element, $|M|^2$, as constant. This contrasts with Beder and Bendix who studied the effects of its variation using a particular isobar model.[14] We, of course, are using the phase-space model only to derive a correction to the experimental data for free nucleons. Presumably the error in neglecting the energy and angle dependences of $|M|^2$ will largely cancel out in the ratio in Eq. (23).

The various kinematic quantities needed to evaluate Eq. (25) for use in Eq. (24) [but not in the denominator of Eq. (23)] may be modified by the nuclear potentials felt by each of the reacting particles. Since each of these particles is, by its nature, a bit different from the others, we must deal with them one at a time.

The incident nucleon as it enters the nucleus will come into an optical potential. This will change its three-momentum (i.e., its wave number) but not its energy (its frequency). Thus, comparing the incident nucleon four-momenta inside and outside the nucleus,

$$\begin{aligned} &E_{1,\text{in}}^2 = E_{1,\text{out}}^2 \equiv E_1^2 = p_{1,\text{out}}^2 + m^2 , \\ &p_{1,\text{in}}^2 = (E_1 - V_1)^2 - m^2 \neq p_{1,\text{out}}^2 , \end{aligned} \tag{26}$$

where V_1 is taken as the real part of the optical potential. We will assume the simple form[15]

$$V_1 = -(2\pi/E_1)\rho \,\text{Re} f_{NN,\text{lab}}(0) , \tag{27}$$

which, at our energy of 740 MeV, gives[9]

$$V_1 \approx +26 \text{ MeV} . \tag{28}$$

The nucleon will slow down somewhat as it enters the region of this repulsive potential.

The initial, bound nucleon with three-momentum $\vec{k}$ has an energy

$$E_2 \equiv k_0 = (m^2 + \vec{k}^2)^{1/2} + V_2 \tag{29}$$

[compare with Eq. (26)]. The potential V_2 is such that the "last" nucleon (i.e., one with $|\vec{k}| = k_F$) is bound by $B = 8$ MeV. Thus

$$\begin{aligned} V_2 &= m - (m^2 + k_F^2)^{1/2} - B \\ &\approx -\frac{k_F^2}{2m} - B . \end{aligned} \tag{30}$$

We will neglect the relatively small optical potentials seen by the two final nucleons. This is because they have, on the average, energies intermediate to that of the bound nucleon ($V_2 < 0$) and the incident one ($V_1 > 0$), i.e., energies near where the potential changes sign. To do otherwise, incidentally, would introduce another integration over the relative momentum of the final NN system.

Finally, we face the question of whether or not the created pion feels an optical potential, at least as far as the evaluation of Eq. (25) is concerned. Beder and Bendix[4] have claimed it does, and evaluate $p_{\pi,\text{lab}}$ using a formula like Eq. (26) and a potential V_π taken from Ref. 15.[16] We claim, however, that $p_{\pi,\text{lab}}$ should *not* be corrected for such a potential. For, the production is assumed here to take place at a point.[17] At the moment of its creation, the pion is interacting with the two nucleons that created it but is far away from all the other nucleons in the nucleus.[18] Thus the pion-nucleon multiple scatterings that give rise to the optical potential have not yet had time to take place so as to modify $p_{\pi,\text{lab}}$ to its "inside" value. Thus we will use the "outside" (or, free) value

$$p_{\pi,\text{lab}} = (E_{\pi,\text{lab}}^2 - \mu^2)^{1/2} = (2\mu T + T^2)^{1/2} \tag{31}$$

in evaluating Eq. (25).

We admit that this point is a troublesome one and that the logic that leads us to Eq. (31) is rough at best. Let us, however, make the following additional comments:

(1) Had we used an "inside" $p_{\pi,\text{lab}}$, as in Eq. (26), we would be overcounting the interactions of the pion with the nucleons that create it. These effects are already present and accounted for in the free-production cross section that is to be multiplied by the $F(T, \theta)$ of Eq. (23).

(2) If we *were* to evaluate the $F(T, \theta)$ using an "inside" $p_{\pi,\text{lab}}$ (but without any factor of $\frac{1}{2}$[16]), then the fitting procedure described in Sec. III E below would lead to a wild behavior for $\sigma_{\pi,\text{abs}}(T)$. It would be 47 mb at 105 MeV, zero at 155 MeV, and *negative* at energies above that. The reason for this is that a modified $p_{\pi,\text{lab}}$ affects the spectrum strongly, cutting it off (at $\theta = 15°$) well before the free-reaction cutoff.

(3) Indeed, it is our feeling that most of the strong variations from the free-phase-space spectrum shown in Fig. 1 of Ref. 4 arise not from the Fermi averaging or the nucleon potentials but from using a $p_{\pi,\text{lab}}$ modified by the potential. As will be seen

below, a comparable figure for our situation shows smaller changes.

(4) For calculating an absorption process $\pi NN \to NN$ as it occurs within the nuclear medium,[19] we *would* use the $p_{\pi,\mathrm{lab}}$ as modified by V_π, since the pion will have had sufficient time to adjust to the medium before the reaction takes place. This asymmetry is not in contradiction with time-reversal invariance, inasmuch as this invariance only makes statements regarding the matrix element M, not the flux or phase-space factors. In our model M is taken as a constant.

The calculation of the quantities W_{NN} and $k_{NN} = (\frac{1}{4}W_{NN}^2 - m^2)^{1/2}$ in Eq. (25) is complicated somewhat by the presence of the nuclear potentials V_1 and V_2. To work out the invariant

$$W_{NN}^2 = (E_1' + E_2')^2 - (\vec{p}_1' + \vec{p}_2')^2 \tag{32}$$

we will use energy and momentum conservation to express things in terms of the known (laboratory) quantities $p_1 = (E_1, \vec{p}_{1,\mathrm{in}})$, $p_2 = (E_2, \vec{p}_{2,\mathrm{in}}) \equiv (k_0, \vec{k})$, and $p_\pi = (E_\pi, \vec{p}_\pi)$. Energy conservation gives at once

$$E_1' + E_2' = E_1 + k_0 - E_\pi , \tag{33}$$

ignoring the small energies of the heavy nuclear residua. We cannot ignore the *momenta* carried by those residua, however. The initial momenta are along the z direction and satisfy

$$\vec{p}_{1,\mathrm{out}} = \vec{p}_{1,\mathrm{in}} + \vec{p}_{\mathrm{nucleus}},$$
$$\vec{p}_{\mathrm{nucleus}} = \vec{p}_{\mathrm{residuum}} + \vec{k}. \tag{34}$$

We now invoke the impulse approximation, that the momentum of the residuum is unchanged by the production reaction,

$$\vec{p}'_{\mathrm{residuum}} = \vec{p}_{\mathrm{residuum}} . \tag{35}$$

With this the momentum-conservation equation,

$$\vec{p}_{1,\mathrm{in}} + (\vec{k} + \vec{p}_{\mathrm{residuum}}) = \vec{p}_1' + \vec{p}_2' + \vec{p}_\pi + \vec{p}'_{\mathrm{residuum}} ,$$

becomes

$$\vec{p}_1' + \vec{p}_2' = \vec{p}_{1,\mathrm{in}} + \vec{k} - \vec{p}_\pi . \tag{36}$$

Thus we can now evaluate the right-hand side of Eq. (32). This gives the same W_{NN}^2 as would be obtained by a naive use of four-momentum conservation but ignoring the initial and final nuclear residua:

$$W_{NN}^2 = (p_1' + p_2')^2 = (p_1 + p_2 - p_\pi)^2 , \tag{37}$$

evaluating the four-momentum dot products using the "inside" momenta and bound-state energies where appropriate.

Throughout the calculation we neglect small Coulomb potentials, so that $F(T, \theta)$ is the same for all nuclei and all pion charges. The error here is worst for the highest Z nucleus. We have explicitly carried out the calculation of $F(T, \theta)$ with Coulomb contributions appropriate for Pb included and have found that the changes are always less than 15%.

Figure 1 shows the phase-space-model pion spectrum for the free case (a), when the Fermi average is taken (b), and when both the Fermi motion and the nucleon optical potential V_1 are included (c). We make the following comments:

(1) The Fermi average alone with $k_F = 250$ MeV/c reduces the cross section $d^2\sigma/dTd\Omega$ quite a bit in the energy region accessible to a free nucleon. It also produces a high-energy tail extending above the cutoff for the reaction involving free nucleons. Not shown in Fig. 1 is the effect of changing k_F by ± 50 MeV/c. This would change curve (b) by some $\pm 25\%$ at most and extend or contract the tail.

(2) The effect of turning on the repulsive potential V_1 is to raise the curve to (c) and extend it to a higher cutoff. The scale increase is largely due to the decrease in the invariant flux factor $[(p_1 \cdot p_2)^2 - p_1^2 p_2^2]^{1/2}$ due to the incident nucleon slowing down. The higher cutoff is a bit more surprising. It comes about because, with a smaller incident three-momentum the heavy particles in the final state do not need to carry away so much three-momentum to balance the budget. This means there is more kinetic energy available to the produced pion than in the case when V_1 is zero.

(3) The correction factor $F(T, \theta)$ is, of course, the ratio of curve (c) to curve (a). Figure 1 shows only the case for production at $\theta = 15°$, but the curves for other angles are similar. $F(T, \theta)$ is

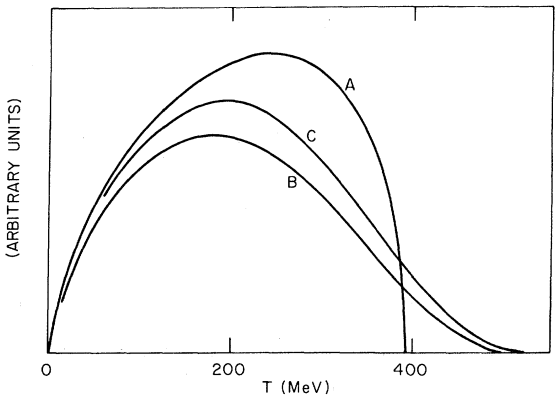

FIG. 1. Phase-space-model predictions for the pion spectrum in the reaction $NN \to NN\pi$ at $\theta = 15°$ and an incident proton energy of 740 MeV: (a) case of reaction on free nucleons; (b) effect of averaging over Fermi motion; (c) effects of Fermi average and potential for the incident nucleon. Values chosen for k_F, B, and V_1 are 250 MeV/c, 8 MeV, and 26 MeV, respectively.

typically between 0.6 and 0.9. [For energies above the nominal free cutoff we arbitrarily set $F(T, \theta) = 1$, to allow for some energy spreads in the experimental data.]

D. Pion-Charge-Exchange Cross Section

The free πN charge-exchange cross section, $\sigma_{\pi,\mathrm{exch}}(T)$, varies rapidly in the energy region of interest, so that Fermi averaging may have substantial effects here also. As with the *pn* charge exchange (Sec. III B), the Pauli principle will tend to cut down the forward scattering and should therefore also be included. Finally, we should include the effects of the pion potential since, in this case, the pion will have traveled some distance through the nuclear medium before the charge-exchange scattering.

Since our model assumes straight-line pion paths, one might argue that only the small angle part of $\sigma_{\pi,\mathrm{exch}}$ should be used in Eq. (4). However, the charge-exchange process "conserves" the number of pions even though it can scatter them well out of their initial energy and angle bins. Thus we use the *total* charge-exchange cross section in our calculations. Our model, as a result, can be expected to work better for predictions of *total* pion-production cross sections than for angular distributions or pion-energy spectra.

We therefore carry out an integration over all scattering angles:

$$(\sigma_{\pi,\mathrm{exch}})_{\mathrm{ave}} = \frac{3}{4\pi k_F^{\,3}} \int d^3k \int d\Omega \left(\frac{d\sigma_{\pi,\mathrm{exch}}}{d\Omega}\right)_{\mathrm{free}} \Theta . \tag{38}$$

For the free cross section we will assume a (3, 3)-dominated resonance amplitude, so

$$\left(\frac{d\sigma_{\pi,\mathrm{exch}}}{d\Omega}\right)_{\mathrm{free}} = \frac{2}{9}\,\frac{\sin^2\delta(q)}{q^2}\,(1+3\cos^2\theta_{\mathrm{c.m.}}) . \tag{39}$$

Here $\theta_{\mathrm{c.m.}}$ is the scattering angle in the πN c.m. frame and q is the c.m. momentum, a function of $\vec{k}$ as well as T (and $p_{\pi,\mathrm{in}}$). For $\sin\delta(q)$ we use the "Breit-Wigner shape with two radii,"[20] for which

$$\tan\delta = M_\Delta \Gamma(q)/(M_\Delta^{\,2} - W^2) , \tag{40a}$$

$$W^2 = p_\pi^{\,2} + 2\,p_\pi \cdot p_N + p_N^{\,2} , \tag{40b}$$

$$q^2 = [(p_\pi \cdot P_N)^2 - p_\pi^{\,2} p_N^{\,2}]/W^2 . \tag{40c}$$

The last two equations are written in terms of four-vector dot products.

The factor Θ in Eq. (38) incorporates the Pauli principle. It is 1 when the final-nucleon three-momentum in the laboratory, $\vec{k}'$, satisfies $|\vec{k}'| > k_F$ and is zero otherwise. As in Sec. III B,

$$|\vec{k}'| = (k^2 + 2\vec{k}\cdot\vec{Q}_L + Q_L^{\,2})^{1/2} , \tag{41}$$

where the laboratory momentum transfer $\vec{Q}_L$ can be obtained from the c.m. four-momentum transfer

$$\begin{aligned} Q_{\mathrm{c.m.}}^{\ \mu} &= (q - q')^\mu = (0, \vec{Q}_{\mathrm{c.m.}}) , \\ Q_{\mathrm{c.m.}}^{\ 2} &= 2q^2(1 - \cos\theta_{\mathrm{c.m.}}) , \end{aligned} \tag{42}$$

by a Lorentz transformation with velocity

$$\vec{\beta} = \frac{\vec{p}_{\pi,\mathrm{in}} + \vec{k}}{E_\pi + k_0} . \tag{43}$$

The formula for $|\vec{k}'|$ is somewhat complicated so we decline to give it here.

The last equation already indicates one way in which the nuclear potentials come in. The Fermi average in Eq. (38) also implies the existence of a nuclear potential for the bound nucleon. We will again use Eqs. (29) and (30) to obtain the four-vector $p_N = (k_0, \vec{k})$. The four-vector for the pion, $p_\pi = (E_\pi, 0, 0, p_{\pi,\mathrm{in}})$ could be found using formulas analogous to Eqs. (26) and (27), together with an appropriate energy-dependent resonance amplitude $f_{\pi N}(0)$. In such a case, however, the potential V_π would be so attractive below resonance that it would force, at some energies, the square of the pion's effective mass, $\mu^{*2} = E_\pi^{\,2} - p_{\pi,\mathrm{in}}^{\,2}$, to become negative, which is mildly perplexing.[21,22]

As has recently been stressed,[11,23-26] it is more appropriate to solve for the pion three-momentum inside the nucleus in a self-consistent way. Consequently, we solve the dispersion relation

$$P_\pi^{\,2} - 4\pi\rho f_{\pi N}(P_\pi, E_\pi) = p_\pi^{\,2} = E_\pi^{\,2} - \mu^2 \tag{44}$$

for $p_{\pi,\mathrm{in}} = \mathrm{Re}P_\pi$.[27] All quantities here are in the laboratory frame. Following Ericson and Hüfner[23] (and ignoring the ambiguities of what off-shell extrapolation is to be taken[24]), we shall simply assume, in the spirit of Chew-Low,[11]

$$f_{\pi N}(P_\pi, E_\pi) = \frac{C P_\pi^{\,2}}{(E_R - E_\pi - i\,\Gamma/2)} . \tag{45}$$

Here C and Γ will be taken as *constants* necessary to fit the total (averaged) πN cross section. We find

$$\begin{aligned} p_{\pi,\mathrm{in}}^{\ 2} &= p_\pi^{\,2} f(x) , \\ f(x) &= \frac{1}{2}\left[1 + \frac{\alpha x}{1+x^2} + \left(1 + \frac{\alpha(2x+\alpha)}{1+x^2}\right)^{1/2}\right] , \\ x &= \frac{E_R - 4\pi\rho C - E_\pi}{\Gamma/2} , \\ \alpha &= \frac{4\pi\rho C}{\Gamma/2} . \end{aligned} \tag{46}$$

Graphs of $f(x)$, $p_{\pi,\mathrm{in}}$, and $\mu^{*2} = E_\pi^{\,2} - p_{\pi,\mathrm{in}}^{\,2}$ versus T are shown in Fig. 2. Note that, with this prescription, $\mu^{*2} > 0$ at all energies, although at times just barely so. The effect of the pion potential,

attractive below resonance and repulsive above, can be seen in the crossover in curve (b). This crossover is, in this simple model, downshifted from the free resonance peak by $4\pi\rho C = 76$ MeV.[23,28]

We mention in passing that if, as assumed here, the pion feels a *large* potential as it moves inside the nuclear medium, the assumption of straight-line pion paths becomes suspect. There could well be large refractive effects at the surface as the pion comes out into the vacuum. We have ignored these throughout, particularly since, after its creation and while the pion is adjusting to the nuclear medium, there will also be (even nastier) refractive effects.

The results of carrying out the (fourfold) integrations in Eq. (38) are shown in Fig. 3. Curve (a) shows the free-charge-exchange cross section obtained from Eq. (39). Including the effects of the Fermi average and the Pauli principle but not the pion potential gives curve (b); the area under this curve is about 67% of that under (a). Not shown is a curve for the Fermi average alone, rather similar to curve (b) but generally larger and less scooped out at the low energies, with area 86% of curve (a). Finally, the full calculation including the pion potential is shown in curve (c). The result of these averages is an upshifted peak,[29] whose integrated strength is some 83% of the free peak.

We wish to emphasize that there is quite a bit of ambiguity in these calculations, particularly with respect to the choice made for $f_{\pi N}$ in Eq. (44).[24] As we shall see, however, in the extraction of the fitted $\sigma_{\pi,\mathrm{abs}}(T)$ discussed below and in the resulting predictions for pion production, it makes little difference if V_π is present or not.[30]

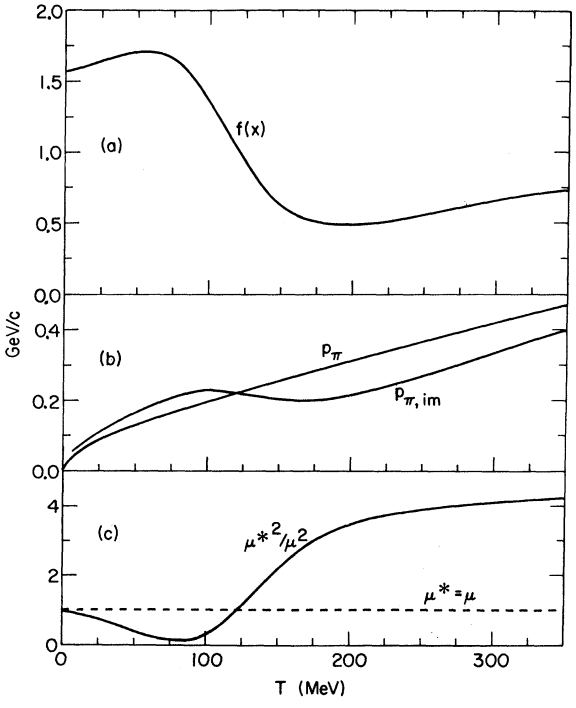

FIG. 2. Effects of the pion potential on pion kinematics: (a) function $f(x)$ of Eq. (46); (b) $p_{\pi,\mathrm{in}}$ and $p_\pi = (E_\pi^2 - \mu^2)^{1/2}$ versus T; (c) effective pion mass squared, $\mu^{*2} = E_\pi^2 - p_{\pi,\mathrm{in}}^2$, in units of μ^2.

E. Pion-Absorption Cross Section

The last input cross section needed is $\sigma_{\pi,\mathrm{abs}}(T)$, about which there is no useful experimental information. Consequently, as in I, we adopt an empirical procedure to determine it.

Presumably the effect of pion absorption is greatest for heavy nuclei and the error from neglect of multiple scattering is least for small-angle π^+ production. Thus, with all the other input cross sections as described above, we can evaluate the differential cross section using Eq. (14) and adjust $\sigma_{\pi,\mathrm{abs}}(T)$ to reproduce the measured $d^2\sigma(\pi^+)/dTd\Omega$ for Pb at 15°. This is exactly the same procedure used in I except that now $\sigma_{N,\mathrm{abs}}$ is a known quantity, not a fitted one.

Curve (a) of Fig. 4 shows the results obtained for this fit using all of the input cross sections and their corrections as discussed in Secs. III A through III D. The cross section shows, not unreasonably, a broad resonance-like peak centered at 200 MeV.

A similar fit to $\sigma_{\pi,\mathrm{abs}}(T)$ but with *no* pion-potential correction to $\sigma_{\pi,\mathrm{exch}}$ gives numbers which differ by less than 7% from those shown in curve (a) of Fig. 4.

The fit to $\sigma_{\pi,\mathrm{abs}}$ obtained in I is shown, for comparison, as curve (b) of Fig. 4. There is quite a difference with even the qualitative nature of the

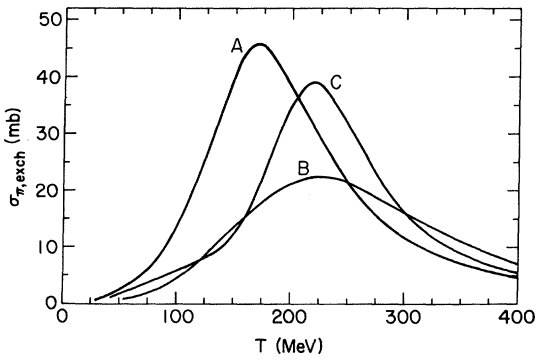

FIG. 3. Pion-charge-exchange cross sections as a function of pion energy: (a) both pion and nucleon free; (b) effects of Fermi average and the Pauli exclusion principle, $k_F = 250$ MeV/c; (c) effects of Fermi average, Pauli principle, and the pion "potential" (see text).

old fit without any nuclear-medium corrections. This fit corresponded to taking $\sigma_{N,\,\mathrm{abs}} = 30$ mb. If we were to arbitrarily set $\sigma_{N,\,\mathrm{abs}} = 25$ mb instead of 5.6 mb [Eq. (19)], recalling that some 3.1 mb of additional absorption is now present because of $\sigma_{N,\mathrm{exch}}$, and again fit $\sigma_{\pi,\,\mathrm{abs}}(T)$ with everything else as discussed above, then we would get the fit shown in curve (c). Except for the turnover due largely to $F(T, \theta)$ being less than 1 at the larger pion energies, there is a vague resemblance to curve (b).

Finally, we also show curve (d), which is Beder's prediction for $\sigma_{\pi,\,\mathrm{abs}}(T)$ based on the inverse of the $NN \to NN\pi$ process.[4, 19] The disagreement between this and our extracted $\sigma_{\pi,\,\mathrm{abs}}$ shown in curve (a) is substantial but not so great as in I, where we obtained curve (b).

IV. NUMERICAL RESULTS

Here we will concentrate our attention on the predictions for the total pion-production cross sections for π^+ and π^- for three nuclei, ^{27}Al, ^{63}Cu, and ^{208}Pb. In I we calculated also for the other nuclei studied in the experiment of Ref. 2, and in addition gave extensive graphs of results for angular distributions and energy spectra.[31] As will be seen from the total cross sections to be presented (which are the quantities most reliably calculated in this model), the *qualitative* nature of the fits in I is not changed much by the nuclear corrections considered here. In general the quality of the angular distributions and energy spectra is similar to that found in I and we will not consider these quantities any further.

The results comparing a number of different calculations for 740-MeV incident protons with each other and with experiment[2] are given in Table I. We make these comments:

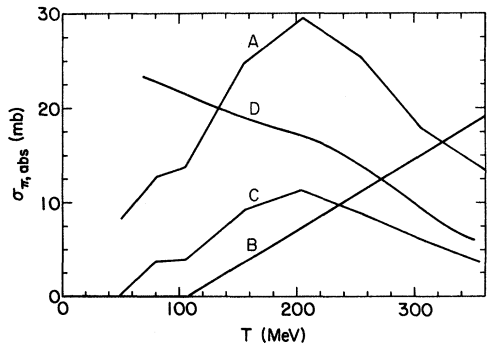

FIG. 4. Fits to $\sigma_{\pi,\,\mathrm{abs}}(T)$: (a) full calculations, all considered nuclear corrections; (b) old fits from Ref. 1, with no nuclear corrections (here $\sigma_{N,\,\mathrm{abs}} = 30$mb); (c) as in (a) but with $\sigma_{N,\,\mathrm{abs}} = 25$ mb instead of 5.6 mb; (d) prediction by Beder (Ref. 19).

(1) For the present calculation, part (c) of the table [viz. Table I (c)], the π^+ cross sections are low for the light nuclei and about right for Pb. In contrast, the results from I [in Table I(b)], have the π^+ cross section about right for Al and somewhat large for Cu and Pb.
(2) For π^- production, we predict cross sections for all three elements which are too small. In the earlier calculation for Pb we had a cross section larger than experiment.
(3) As a result of (1) and (2), the present π^+/π^- ratios are not as good as before. We now have too much π^+ production for the heavy elements, in spite of the reduction due to nucleon charge exchange. This is probably because of the larger $\sigma_{\pi,\,\mathrm{abs}}$ here (as compared with I), which tends to decrease the probability of a pion escaping from the interior of the nucleus.

TABLE I. Predictions for total π^+ and π^- production cross sections for Al, Cu, and Pb at an incident proton energy of 740 MeV. The $\sigma(\pi^\pm)$ are in mb while R, r_0, and a are in fm. The Saxon-Woods parameters are taken from Ref. 6, those for Cu being obtained from the parameters for nearby Ni.

	Al	Cu	Pb
(a) Experiment, taken from Ref. 2.			
$\sigma(\pi^+)$	53.1 ±2.9	77.3 ±4.3	104.2 ±5.8
$\sigma(\pi^-)$	13.2 ±0.9	25.2 ±2.0	53.7 ±4.9
$\sigma(\pi^+)/\sigma(\pi^-)$	4.02±0.35	3.07±0.30	1.94±0.21
(b) Predictions from Ref. 1, uniform sphere density, no nuclear charge exchange, no nuclear corrections.			
R	3.78	4.97	7.11
$\sigma(\pi^+)$	50.9	82.0	128.9
$\sigma(\pi^-)$	12.5	25.4	64.3
$\sigma(\pi^+)/\sigma(\pi^-)$	4.07	3.23	2.00
(c) Present model, Saxon-Woods density, nuclear charge exchange, and nuclear corrections of Sec. III.			
r_0	3.07	4.14	6.66
a	0.52	0.57	0.50
$\sigma(\pi^+)$	40.4	65.4	108.2
$\sigma(\pi^-)$	9.9	18.8	45.6
$\sigma(\pi^+)/\sigma(\pi^-)$	4.07	3.47	2.37
(d) Same as (c) but with no V_π correction.			
$\sigma(\pi^+)$	40.5	65.4	108.6
$\sigma(\pi^-)$	9.6	18.1	43.8
$\sigma(\pi^+)/\sigma(\pi^-)$	4.22	3.61	2.48
(e) Same as (c) but with $\sigma_{N,\,\mathrm{abs}} = 25$ mb.			
$\sigma(\pi^+)$	36.9	59.9	100.1
$\sigma(\pi^-)$	9.2	17.7	44.3
$\sigma(\pi^+)/\sigma(\pi^-)$	3.99	3.38	2.26

(4) Table I(d) shows the predictions when the pion potential correction is *not* made for $\sigma_{\pi,\text{exch}}$. As expected, since the fitted $\sigma_{\pi,\text{abs}}(T)$ values are essentially unchanged (see Sec. III E), the $\sigma(\pi^+)$ predictions are hardly different from the case with V_π included [part (c)]. The π^- production is now a little smaller since there is less charge exchange for the pion transport [compare curves (b) and (c) of Fig. 3]. Thus the π^+/π^- ratios are slightly worse than with V_π included.
(5) Table I(e) shows the results when $\sigma_{N,\text{abs}}$ is arbitrarily increased to 25 mb (an absorption like that used in I). The production is now smaller than before, with the change in the π^- production less than in the π^+ production. The difference is related to the smaller $\sigma_{\pi,\text{abs}}$ used [compare curves (a) and (c) of Fig. 4]. Even so, the π^+/π^- ratios do not come down to the experimental values.

To see how and where the changes between Table I(b) and I(c) arise, we give in Table II the effects of turning off each of the corrections made in the present calculation, one at a time. Each change is compared with a "standard calculation," that for Pb. We comment on each of these changes in turn:
(1) The changes due to neglecting the corrections to $\sigma_{\pi,\text{exch}}$ are small and in the expected direction. For here there is more pion charge exchange [compare curves (a) and (c) of Fig. 3] and thus more π^- production.
(2) The changes due to neglecting the corrections to $d^2\sigma/dTd\Omega$ are large. (Note that $\sigma_{\pi,\text{abs}}$ has not been refitted in the numbers presented.) This is illustrated in Fig. 1, where the area under curve (a) is some 18% larger than that under curve (c). Evidently the differences are correspondingly larger for angles greater than 15°.
(3) The changes due to neglecting the Pauli-principle correction to $\sigma_{N,\text{exch}}$ (i.e., using $\sigma_{N,\text{exch}} = 3.8$ mb instead of 3.1 mb are negligible in π^+ production (slightly more absorption) and increase the π^- production slightly. As stated above, it is easier for neutrons to make π^- than for protons. The π^+/π^- ratio is still greater than experiment.
(4) Dropping $\sigma_{N,\text{exch}}$ altogether makes large changes in π^- production, with the π^+/π^- ratio now very much larger than experiment.
(5) Going from the Saxon-Woods nuclear density, Eq. (3), to a sharp-edged uniform density with the same r.m.s. radius gives relatively minor changes, mostly for the π^+ production. This leads to the conclusion that any detailed information on the nuclear density will be masked by the other,

TABLE II. Effects of the various corrections (considered one at a time) on the calculated Pb total production cross sections. Again, the incident proton energy is 740 MeV. All cross sections are in mb.

$\sigma(\pi^+)$	% Change	$\sigma(\pi^-)$	% Change	$\sigma(\pi^+)/\sigma(\pi^-)$	% Change
(a) Experiment, taken from Ref. 2.					
104.2 ± 5.8	···	53.7 ± 4.9	···	1.94 ± 0.21	···
(b) "Standard calculation," Saxon-Woods density with $r_0 = 6.66$ fm and $a = 0.50$ fm, nucleon charge exchange, and all nuclear corrections of Sec. III.					
108.2	···	45.6	···	2.373	···
(c) Same as (b) but without Fermi averaging, Pauli principle, and pion-potential corrections for $\sigma_{\pi,\text{exch}}$.					
105.2	−2.8	49.8	+9.2	2.113	−11.0
(d) Same as (b) but without Fermi averaging and nucleon-potential corrections for $d^2\sigma_{\text{iso}}/dTd\Omega$.					
193.1	+78.5	62.0	+35.9	3.116	+31.3
(e) Same as (b) but without Pauli-principle correction for $\sigma_{N,\text{exch}}$, i.e., $\sigma_{N,\text{exch}} = 3.8$ mb.					
107.2	−1.0	47.9	+5.0	2.238	−5.7
(f) Same as (b) but with no nucleon exchange at all, $\sigma_{N,\text{exch}} = 0$.					
114.0	+5.4	34.1	−25.2	3.341	+40.9
(g) Same as (b) but with sharp-edged uniform sphere density of radius $R = 7.11$ fm.					
92.4	−14.6	43.6	−4.4	2.117	−10.8

more significant (and somewhat ambiguous) nuclear corrections.

It is probably worth mentioning once again at this point that our predictions depend seriously on the assumption of a rather simple isobar model.[5] As already indicated, there are reasons to suspect its validity.[10] It could well be that our present results are not in better agreement with experiment because of this. If a complete set of pion spectra were available for the other $NN \to NN\pi$ reactions at the desired energy, then our model would become independent of these particular assumptions.

Finally, we check the oft-claimed statement that, at least for the π^+ case, most of the pion production occurs in the nuclear surface.[3,4] We have segmented the Saxon-Woods nucleus as shown in Fig. 5. In a "standard calculation" for Pb we then kept track of the segment, or bin, in which the pion that eventually emerges as a π^+ or π^- is created. The various bin contributions to $\sigma(\pi^+)$ and $\sigma(\pi^-)$ are listed in Table III. As can be seen, most (75.7%) of the π^+ production does come from the regions where $\rho \leq 0.9\rho_0$, especially from the annulus (bin 2). In fact, from calculations not shown in Table III, 41.6% of the π^+ production comes from even thinner regions where $\rho \leq 0.5\rho_0$. For π^- production, on the other hand, the production is more evenly distributed over the six bins. There is still a lot of production in the annulus but now 34.3% of the π^-'s originate in the core ($\rho \leq 0.9\rho_0$). This is in accord with the notion emphasized here that π^-'s are not made directly but more through secondary charge-exchange reactions. Thus we see that the picture of surface production is only approximately correct.

V. SUMMARY

In this paper we have given careful attention to how a rather successful, almost classical model of pion production from nuclei at intermediate energies could be extended to take into account a number of nuclear effects. A motivation for this was the hope of learning something new about the nuclear density. We have seen, however, that the differences in predicted production cross sections due to the drastic change from a Saxon-Woods to a uniform density were generally much smaller than those due to including other nuclear corrections. Perhaps the relative insensitivity to the nuclear density could have been expected from the data of Cochran *et al.*[2] The existence of simple scaling laws for total and differential cross sections would imply that rather gross geometrical effects predominate.

On the other hand, the corrections due to processes taking place within the nuclear medium are interesting in themselves. A byproduct of this calculation has been the extraction of $\sigma_{\pi,\mathrm{abs}}(T)$, now somewhat more believable than the fit obtained for it in the earlier version of the model. This quantity, of course, is likely to be an important ingredient in many other pion-nucleus interactions and their analyses. It deserves to be better understood. We once again urge our experimental colleagues to provide us with some information regarding this important inclusive process where a pion enters a nucleus and none emerges.

Finally, we should remind the reader that our calculation has three kinds of limitations. The first is the use of a semiclassical model, i.e., the neglect of all quantum mechanical effects.

TABLE III. Origins of produced pions sorted into six nuclear bins according to Fig. 5. This is the "standard calculation" for Pb. All cross sections, partial or total, are in mb.

Bin	$\sigma_i(\pi^+)$	% of π^+	$\sigma_i(\pi^-)$	% of π^-
1	27.2	25.1	8.4	18.5
2	48.7	45.0	17.8	39.0
3	6.1	5.6	3.7	8.1
4	11.1	10.3	5.4	11.7
5	12.3	11.4	7.8	17.1
6	2.9	2.7	2.5	5.5
Totals	108.3	100.1	45.6	99.9

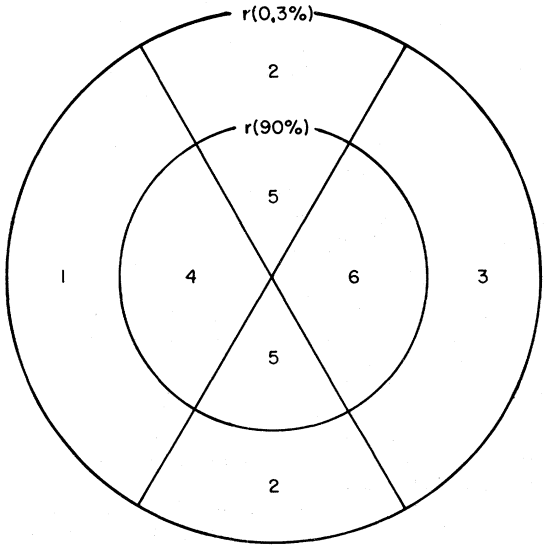

FIG. 5. Division of the nucleus into bins. The case of Pb is illustrated: $r(90\%) = r_0 - 2.2a = 5.6$ fm and $r(0.3\%) = r_0 + 6a = 9.7$ fm, the cutoff radius in the calculation of the integral of Eq. (7).

The second is that, within this semiclassical picture, we treat multiple-scattering effects crudely. This last could be overcome by a Monte Carlo calculation which follows each particle throughout its journey through the nucleus. However, whether one does a quantum mechanical calculation or an improved semiclassical calculation, the third limitation must always be borne clearly in mind. The fact is that the nuclear medium corrections play a large and somewhat uncertain role in modifying the basic interactions. Indeed, until one feels that these corrections are satisfactorily understood, it is probably not sensible to proceed with more elaborate calculations.

As this paper was being prepared for the typist we became aware of the interesting paper by Oganesyan on π^+ and π^- production by 600-MeV *neutrons* on various nuclei.[32] In discussing his experimental results, Oganesyan makes extensive qualitative remarks concerning the role of the absorption, scattering, and charge exchange of the pions (and also the nucleons) in the nuclear matter, as well as other nuclear-structure effects such as Fermi motion.

ACKNOWLEDGMENTS

We have profitted greatly from conversations with H. Bethe, Ching Liang Lin, A. S. Goldhaber, M. Johnson, A. K. Kerman, D. E. Nagle, and G. Stephenson. Much of this work was done or initiated while M. M. S. was a visitor at The Clinton P. Anderson Meson Physics Facility, for which the encouragement and support of L. Rosen is greatly appreciated.

---

*Work supported by the U.S. Atomic Energy Commission.
†Research supported by the National Science Foundation and the U.S. Atomic Energy Commission.

[1]M. M. Sternheim and R. R. Silbar, Phys. Rev. D **6**, 3117 (1972).
[2]D. R. F. Cochran, P. N. Dean, P. A. M. Gram, E. A. Knapp, E. R. Martin, D. E. Nagle, R. B. Perkins, W. J. Shlaer, H. A. Thiessen, and E. D. Theriot, Phys. Rev. D **6**, 3085 (1972).
[3]B. Margolis, Nucl. Phys. **B4**, 433 (1968); R. J. Lombard, J. P. Auger, and R. Basile, Phys. Lett. **36B**, 480 (1971); W. Hirt, Nucl. Phys. **B9**, 447 (1969).
[4]D. S. Beder and P. Bendix, Nucl. Phys. **B26**, 597 (1971). The citation of this reference in I was in error.
[5]For a more complete discussion of the isobar model for $NN \to NN\pi$ and how we use it, see Ref. 1.
[6]H. R. Collard, L. R. B. Elton, and R. Hofstadter, in *Landolt-Börnstein: Numerical Data and Functional Relationships; Nuclear Radii*, edited by K.-H. Hellwege (Springer, Berlin, 1967), New Series, Group I, Vol. 2.
[7]We wish to thank Ching Liang Lin for showing us this method of solution.
[8]Related comments along these lines have been made by D. S. Beder, Can. J. Phys. **49**, 1448 (1971).
[9]See, e.g., the compilation by O. Benary, L. R. Price, and G. Alexander, Lawrence Berkeley Laboratory Report No. UCRL-20000 NN, 1970 (unpublished).
[10]Actually, at $p_{\text{lab}} = 1.39$ GeV/c, i.e., nearly the same energy, $\sigma(pp \to pp\pi^0) = 3.46 \pm 0.25$ mb [R. Cence *et al.*, Phys. Rev. **131**, 2713 (1963)]. This indicates that the simple form of the isobar model we use is somewhat inadequate, but we will ignore the difference for now.
[11]H. Bethe, Phys. Rev. Lett. **30**, 105 (1973).
[12]R. E. Mischke, P. F. Shepard, and T. J. Devlin, Phys. Rev. Lett. **23**, 542 (1969); see also P. F. Shepard *et al.*, Princeton-Pennsylvania Accelerator Report No. PPAR-10, 1969 (to be published).
[13]For example, the *least* momentum transfer to the struck nucleon in $NN \to \Delta N$ is, at our energy, 338 MeV/c. This is larger than the Fermi momentum k_F (but not very much so).
[14]Despite some effort, we were never able to reproduce the phase-space model curve shown in Fig. 1 of Ref. 4.
[15]See, e.g., M. L. Goldberger and K. M. Watson, *Collison Theory* (Wiley, New York, 1964), p. 796.
[16]Goldberger and Watson, Ref. 15, p. 798. Actually, Beder and Bendix used *one-half* the real part of that optical potential. The reason for the factor of (1/2) was because, in their model, pion production takes place largely near the nuclear surface, where the density is more or less half its central value. In our case, with the rather smaller $\sigma_{N,\text{abs}}$ of Sec. III A. this factor of (1/2) would no longer be quite so appropriate.
[17]Even in a two-step process, such as the isobar model, $NN \to N\Delta$, $\Delta \to N\pi$, the Δ only travels $\lesssim 1$ fm before it decays.
[18]The p-wave πN interaction by nucleon exchange in the u channel has a range of ≈ 0.4 fm while the internucleon distance in the nucleus is like $\rho^{-(1/3)} \approx 1.8$ fm.
[19]D. S. Beder, Can. J. Phys. **49**, 1211 (1971).
[20]A. Rittenberg *et al.*, Rev. Mod. Phys. Suppl. **43**, S114 (1971).
[21]For example, an attempt to transform to the pion rest frame in such a case would involve a velocity greater than the speed of light. Indeed, the concept of rest frame is meaningless when $\mu^{*2} < 0$.
[22]The pion's *group* velocity, however, is $p_{\pi,\text{in}}/(E_\pi - V_\pi)$, which is always less than 1 (the speed of light). We thank M. M. Nieto for clarifying this point.
[23]T. E. O. Ericson and J. Hüfner, Phys. Lett. **33B**, 601 (1970).
[24]R. R. Silbar and M. M. Sternheim, Phys. Rev. C **6**, 764 (1972).
[25]S. Barshay, V. Rostokin, and G. Vagradov, Niels Bohr Institute report (to be published).
[26]This idea was proposed and pursued much earlier by R. M. Frank, J. I. Gammel, and K. M. Watson, Phys. Rev. **101**, 891 (1956).
[27]Perhaps more appropriate, in view of the finiteness of the wave train because of the damping in the medium ($\text{Im}P_\pi > 0$), would be to Fourier analyze the wave $\psi = e^{iP_\pi z}$ for the momentum distribution $\varphi(p_{\pi,\text{in}})$. One would then carry out an additional integration in Eq. (38) to average over $|\varphi(p_{\pi,\text{in}})|^2$. We will forgo this complication. We wish to thank H. Bethe and M. Johnson for discussions on this point.
[28]This value is rather larger (about a factor of 2) than that claimed in Ref. 23.
[29]A remark similar to this was made by D. S. Koltun in a talk at the Nuclear Physics Division meeting of the American

Physical Society at Seattle, Washington, in November, 1972.
[30]R. Landau has argued that the Pauli principle will effectively reduce the size of the pion potential (private communication). See also Ref. 11 for comments along this line.
[31]We discovered a minor programming error in the work of Ref. 1, which, when $N \neq Z$, introduced errors of less than 1%.
[32]K. O. Oganesyan, Zh. Eksp. Teor. Fiz. **54,** 1273 (1968) [transl.: Sov. Phys.-JETP **27,** 679 (1968)].